EFFECT OF LOCALISED ELECTRON CYCLOTRON HEATING ON ENERGY CONFINEMENT AND MHD IN TCV

A. Pochelon , Z.A. Pietrzyk, T.P. Goodman, M. Henderson, J-P. Hogge, J-M. Moret,
H. Reimerdes, G. Tonetti, M.Q. Tran, H. Weisen, R. Behn, S. Coda, B.P. Duval, I. Furno,
F. Hofmann, B. Joye, J.B. Lister, X. Llobet, A. Manini, Y. Martin, Ch. Nieswand,
J. Rommers, O. Sauter, W. van Toledo, Y.V. Esipchuk†, A.A. Martynov†,
A. Sushkov† and F. Porcelli*

*Centre de Recherches en Physique des Plasmas, Ecole Polytechnique Fédérale de Lausanne
Association EURATOM-Confédération Suisse, CH-1015 Lausanne, Switzerland
† Russian Research Centre Kurchatov, 12182 Moscow, RF
Politecnico di Torino, Italy

Introduction - This paper reports the effects of localised power deposition on the heating, MHD activity, and confinement in TCV. Initial ECRH studies concentrated on low elongation plasmas, including positive and negative triangularities: this is a necessary step before investigating more strongly shaped plasmas. ECRH power of up to 1 MW at 82.7 GHz (second harmonic X2) was injected, representing up to 14 times the Ohmic power during the heating pulse [1]. When complete, the ECW system will provide 3 MW second harmonic and 1.5 MW third harmonic at pulse lengths of 2 s [2]. For TCV (R = 0.89 m, a = 0.25 m, I_p < 1.2 MA), the nominal field of B = 1.44 T and the frequency of 82.7 GHz place the resonance slightly off-axis on the high-field side (HFS) of the magnetic axis (Δρ=-0.16 to -0.2). This allows us to scan the power deposition location on the HFS, above and below the magnetic axis, on a shot-to-shot basis; or, to sweep it during one shot. Sweeping is done using *1)* steerable launcher mirrors (primarily the poloidal angle θ), *2)* vertical plasma translation in the TCV vessel and *3)* radial displacement of the cyclotron resonance by changing the magnetic field.

The *power deposition location* was determined using the soft X-ray response at the EC shut-off (plus Thomson electron temperature profiles); when not coincident with a sawtooth crash, which perturbed the measurement. The maximum of the power deposition location coincides with the ray tracing prediction to within a few percent in normalised radius ρ, as shown in the example of **Fig. 1**. The low sampling rate of 10 kHz causes the measured deposition profile to appear wider due to the large time window needed for the measurement. The location of the maximum, however, is not affected by the window choice.

Absorption location - The absorption location of the EC power strongly affects the resulting central temperature, confinement and sawtooth behaviour, as shown in **Fig. 2**, depicting a B-field scan (0.5 MW). The deposition is swept across the sawtooth inversion
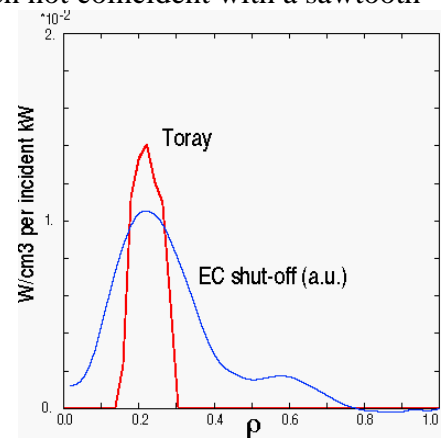

Fig. 1. Typical power deposition from Toray ray tracing (W/cm³ per incident kW) and from soft X-rays at EC shut-off, as a function of normalised radius ρ.

surface (deduced from soft X-ray tomography) on the HFS of the magnetic axis. The *central electron temperature* T_{eo} is maximum for power deposition somewhat inside the sawtooth inversion radius ρ_{inv} (**Fig. 2a**), i.e. towards magnetic axis ($R_{res}-R_{inv}>0$). The *global electron confinement time* τ_{Ee} (**Fig. 2b**) is relatively independent of the resonance position when heating inside ρ_{inv} and drops when heating outside ρ_{inv}, implying efficient heating requires deposition roughly inside ρ_{inv}. Data in **Fig. 2 a, b**) cover a large range of q_a values: $2.3<q_a<6.7$. The *sawtooth period* is maximum for a deposition slightly outside ρ_{inv} (**Fig. 2c**). Note from the Kadomtsev sawtooth-crash reconnection model that $\rho_{q=1}=\rho_{inv}$ for peaked parabolic profiles of T_e and q, and $\rho_{q=1}>\rho_{inv}$ for a flat q profile inside q=1 [3].

Despite the obvious importance of the inversion radius, an additional effect is seen when heating above or below the midplane: central temperature and pressure respond differently to top or bottom q=1 deposition. Relative to on-axis deposition, top q~1 heating produces large normal sawtooth relaxations and degrades central T_{eo}, whereas bottom q~1 heating produces reduced amplitude central relaxations of the humpback type and increases central T_{eo}. The good central performance of bottom q=1 deposition coincides with central relaxations of lower amplitude. This top-/bottom- asymmetry may have its origin in the small co-/counter- current drive component generated even with purely poloidal injection, due to the poloidal magnetic field component arising from the plasma current [4].

Fig. 2. Radial deposition scan through bottom HFS inversion surface, by varying B_φ ($\kappa=1.32$, $q_a=5$, $n_{eo}=2\ 10^{19}[m^{-3}]$, $P_{EC}=360kW$):
a) Relative T_{eo} increase ($2<q_a<6$)
b) Relative global τ_{Ee} degradation
c) Sawtooth period.

Basic confinement dependencies (B, q_a, n_e, P) - A small plasma placed in front of the launcher with a quasi-horizontal launch was studied in order to minimise refraction effects at high density ($\theta=18°$, z=38, $\kappa=1.31$, $\delta=0.15$, $\theta=0°$ is horizontal). Scan domains were: $1.32<B_\varphi<1.45$ T (deposition displacement of 20% of the plasma radius around q=1); 1.5×10^{19} m^{-3} < n_{eo} < overdense; $2.2<q_a<6$; $P_{EC}\approx1$ MW. In the q_a-scan, ratios of P_{tot}/P_{OH} from 3 to 14 were obtained during ECRH with 1MW power injection.

As a function of the *safety factor q_a*, the electron confinement time τ_{Ee} increases with q_a to a maximum at $q_a\sim5$ and drops for $q_a>5$ (**Fig. 3**). In the high q_a shots of this scan ($P_{EC}=500$ kW, $0.77<R_{res}<0.84$ m), the power was deposited outside the inversion surface, which probably explains the drop at high q_a by analogy to the drop observed during the radial B-field scan at constant q_a, when heating outside q=1 (see **Fig. 2b**). **Figure 3** also contains
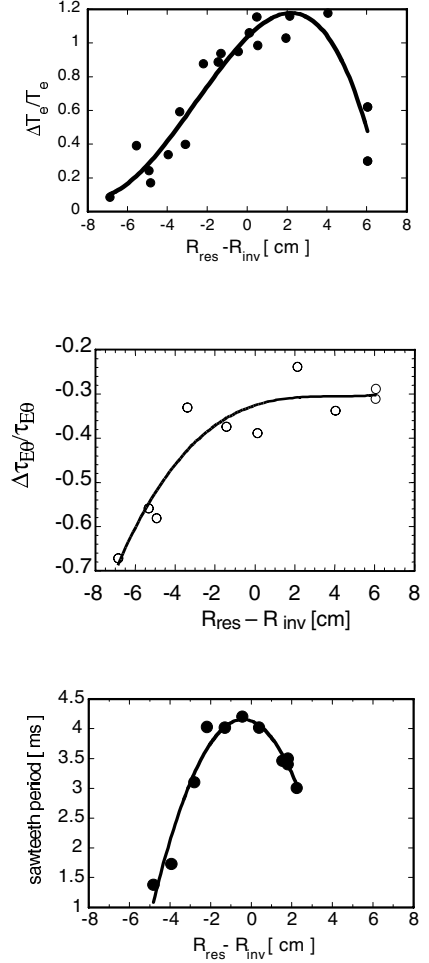
the corresponding ohmic-confinement-time q_a dependence, showing saturation at $q_a > 5$. Even though confinement exhibits the neo-Alcator-like q_a scaling as in ohmic plasmas [5], confinement improvement with q_a is not as high during corresponding ECRH plasmas. It is likely that higher additional power will further degrade the favourable scaling with q_a. In the present heating experiments, however, this beneficial ohmic scaling feature still holds for ECRH power ratios $P_{ECRH} / P_{OH} > 9$.

The dependence of τ_{Ee} as a function of *density* on-axis is shown in **Fig. 4**. Low elongation plasmas ($\kappa=1.16$ and 1.32, $q_a \approx 5$), located in front of the launcher to minimise refraction effects at high density, were chosen for this scan. Stationary density just below cut-off density was not possible to obtain, due to the ECRH-induced density pump-out, explaining the absence of data just below cut-off (TORAY predicts full absorption for $n_{eo} \leq 4.0 \times 10^{19}$ m^{-3}). The confinement time scales linearly with density, as observed in previous low density EC experiments [6].

Power-induced confinement degradation was studied with 1MW of additional power, with a power deposition profile maximum at a radius of $\rho=0.23$. Heating results with $P_{EC} > 500$kW contained a counter-ECCD component for one of the two launchers. This may however be of reduced signi-

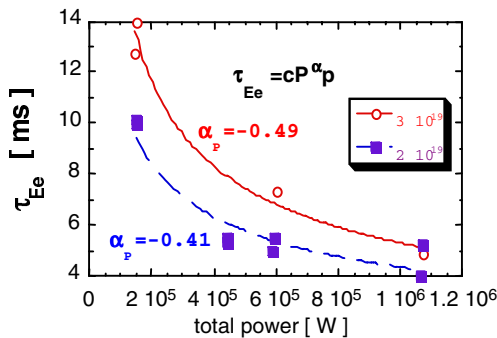**Fig. 3.** τ_r versus q_a, for different deposition radii in a B_φ scan in ECRH, and OH plasmas.

Fig. 4. τ_{Ee} as a function of n_{eo} for two elongations ($\kappa=1.16$, 1.32; $\delta=0.07$, 0.16, $q_a=4.7$, 5.2)

ficance on confinement, since power degradation in ECCD was observed to be similar to ECRH [7]. The power-induced degradation exponent α_P, ($\tau_{Ee} \sim P^{\alpha_P}$), measured for $q_a=5$ at $n_e=2$ and 3×10^{19}m^{-3} (see **Fig. 5**), and at $q_a=2.5$ for a density close to 2×10^{19} m^{-3}, is as usual: $\alpha_P \sim -0.5$, or possibly somewhat lower. Note that this confinement degradation may have been favourably influenced by the effect of slightly off-axis heating on profiles and MHD-activity. In particular, the sawtooth

Fig. 5. τ_{Ee} power degradation for two densities, $q_a=5$.

period is lengthened for a deposition close to $q=1$, and when raising the power, sawtooth activity is observed to convert to humpback relaxations before disappearing at the higher powers.
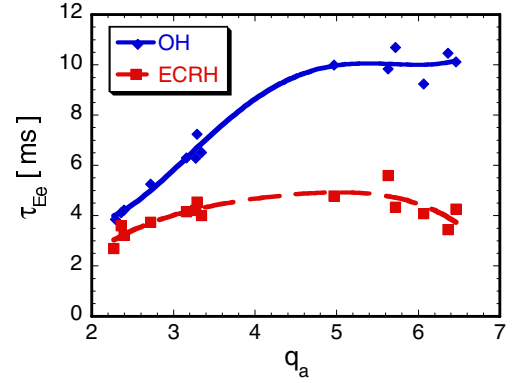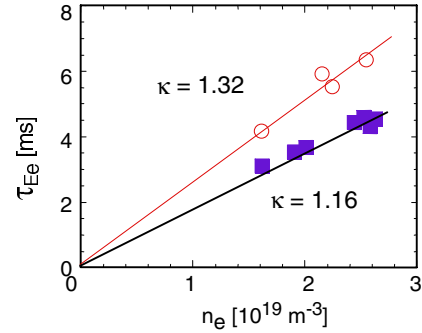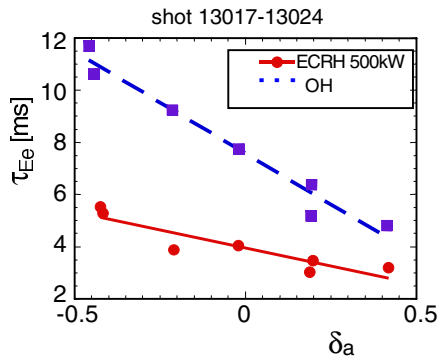
Fig. 6.
τ_{Ee} as a function of δ, ohmic and ECRH data.
(P_{EC}=500 kW, κ=1.32,
q_a=3.5 (227<I_p<255 kA), n_{eo}=2 10^{19} [m^{-3}]).

Plasma shape: triangularity - The study of confinement with triangularity was done with medium q_a, q_a=3.5, at 500kW. The power was also deposited close to the inversion surface. Both ECRH and ohmic cases are shown in **Fig. 6**. As with ohmic heating, confinement improves with increasing negative triangularity during ECRH. Note that from this scan, the improvement of confinement with ECRH appears less than with purely ohmic heating. The real trend however is probably more favourable with negative triangularity than shown here, since power deposition occurred inside ρ_{inv} for δ>0 and outside ρ_{inv} for δ<0 (recall **Fig. 2b**).

Conclusions - Confinement, central heating and MHD-activity depend strongly on the location of the EC power deposition. Sawteeth periods are the longest for power deposition just outside ρ_{inv} and mode activity is enhanced for deposition inside ρ_{inv}. Dramatic increases in central electron temperature T_{eo} occur when power is deposited close to ρ_{inv} on the HFS or below midplane; small amplitude central relaxations of humpback type also occur here.

Within the range of plasma shapes and plasma currents investigated, the electron confinement time, τ_{Ee}, increases with safety factor, density and negative triangularity similar to the Ohmic heating case. There is little dependence of τ_{Ee} on the heating location provided power deposition occurs inside the q=1 surface; as power deposition moves out of the inversion surface, τ_{Ee} decreases. The power-induced energy confinement degradation exponent ($\tau_{Ee} \sim P^{\alpha_P}$) is as usual: $\alpha_P \sim$ -0.5. As a general trend, central relaxations decrease in amplitude with increasing q_a, P_{EC}, or negative δ, in a situation where the confinement time increases.

Acknowledgement

References

[1] A. Pochelon et al.: *2nd Eur. Top. Conf. on RF Heating and Current Drive of Fusion Devices*, Brussels, **22A**, 253 (1998).

[2] T.P. Goodman et al.: *Proc. EC-10 Conf.*, Ameland, 305 (1997).

[3] Z.A. Pietrzyk et al.: *this Conference*.

[4] T.P. Goodman et al.: *this Conference*.

[5] J.-M. Moret et al.: PRL **79**, 2057 (1997); H. Weisen et al.: NF **37**, 1741 (1997).

[6] V.V. Alikaev et al.: *10th Int. Conf. on Plasma Phys. Cont. Nucl. Fus.*, **I**, 419 (1985).

[7] Y. Esipchuk: Plasma Phys. and Contr. Fus. **37**, Suppl. 11A, A267 (1995).